Ocean Engineering 129 (2017) 46–56

Contents lists available at ScienceDirect

Ocean Engineering

journal homepage: www.elsevier.com/locate/oceaneng

Connection effect on amplitude death stability of multi-module floating airport

H.C. Zhang[a], D.L. Xu[a,*], C. Lu[b], E.R. Qi[c], C. Tian[c], Y.S. Wu[c]

[a] State Key Laboratory of Advanced Design and Manufacturing for Vehicle Body, Hunan University, Changsha 410082, PR China
[b] SAIC, General Motors Co., Ltd Wuhan Branch, Wuhan 430000, PR China
[c] China Ship Scientific Research Center, Wuxi 214082, PR China

ARTICLE INFO

Keywords:
Multi-module floating airport
Nonlinear network dynamics
Connector
Amplitude death

ABSTRACT

A floating airport consists of multiple floating modules that are serially connected by flexible connectors. A generalized 2D dynamic network model is developed for its dynamic analysis with mooring constraints. Three connection models, including the parallel hinge type, cross hinge type and compound type, are proposed for assessing the performance of dynamic stability in terms of amplitude death that leads to a weak oscillation state. Numerical results illustrate the onset of amplitude death stability of the three models in the parameters domain spanned by the connector stiffness and wave period, in addition with the effect of wave height. The comparison study concludes that the compound type connection may deliver better dynamic stability, which can significantly improve the safety design of multi-module floating airport.

1. Introduction

The research about very large floating structures(VLFS) may trace back to 1924, when Edward R. Armstrong patented the Sea Station to be used as 'aeroplane supply and navigating stations'(Armstrong, 1924). The Sea Station eventually turned into the Armstrong Seadrome, refueling airfields at sea for transatlantic aircraft hauling freight and passengers between the United States and Europe (Armstrong, 1943). But Armstrong's early idea was not accepted due to the high cost and failure to ensure its safety. In the late 1980s,, a number of researchers from industry, academia, and government attempted to initiate substantial research programs in offshore engineering to utilize ocean space. In Japan, the Technological Research Association of Mega-Float (TRAM) was founded in 1995 to conduct research and development on the Mega-Float project (Fujikubo and Suzuki, 2015). A 6-year research project was executed in the aim of developing the fundamental design, construction, and operational technologies in Phase I (1995–1997) and a corroborative study on the use of the Mega-Float as an airport in Phase II (1998–2001)(Isobe, 1999). Different from the pontoon-type proposed by Japanese, the US Navy proposed a Mobile Offshore Base (MOB) concept which consists of several semi-submersible modules with a total length of about 5000 ft in the mid-1999 s (Derstine and Brown, 2000). The mobile offshore base targets multiple purposes. It can either serve as a floating logistics base stationed in coastal or international waters, or several self-propelled modules are connected together to form a runway and support base in sea (McAllister, 1997) for fixed-wing aircraft and helicopters. Apart from the contributions to the research field of VLFS in Japan and USA, specific topics and general areas of the research interest, based upon knowledge accumulated during earlier workshops and conferences (Ertekin and Kim, 1999; Ertekin and Riggs, 1991; Haeda et al., 1996; Suzuki et al., 2007), were abundant all over the world. VLFS have been gradually emerging for applications as floating bridges, floating airport, floating cities, floating fuel storage facilities, etc.(Watanabe et al., 2004). For these massive marine structures, the safety and stability design of VLFS have always been an important topic because it carries many passenger, crews and facilities (Suzuki, 2001).

Multi-module floating structure, connected by connectors, is easy in construction, transportation and deployment (Watanabe et al., 2004). The connector is a key element for the safety design of VLFS. In the early stage of development, rigid connector was proposed to connect multiple floating platforms, but such connection caused extremely large loads in structures (Maeda et al., 1979). In this regard, flexible connectors were adopted, which allow relative motions between floating modules in some degrees of freedom. Xia et al. (2000) dealt with the VLFS as a number of two-dimensional articulated plates connected by idealized connectors as two independent vertical and rotational springs. They showed that the hydroelastic dynamics are strongly dependent on the stiffness of the connectors and the incoming wave frequency. Gao et al. (2011) investigated the effects of the location

* Corresponding author.
E-mail address: dlxu@hnu.edu.cn (D.L. Xu).

http://dx.doi.org/10.1016/j.oceaneng.2016.11.011
Received 17 February 2016; Received in revised form 21 October 2016; Accepted 12 November 2016

and rotational stiffness of the connector for reducing the hydroelastic responses and stress resultants of the VLFS by using Mindlin plate theory. It found that the hinge line connector, when appropriately positioned, is better design compared to a rigid connector. The optimum configuration of a modular floating structure with flexible connectors, modeled as two linearized springs in longitudinal and/or transverse directions, was investigated by Michailides et al. (2013). The analysis results of three grid types of the floating structure showed that the change of the grid type (number and layout of modules) affects directly the connectors' internal loads and the modules responses. Above research works are all about pontoon type floating structure. In order to reduce the hydrodynamic responses, semi-submersible type floating platform is proposed. The motion responses and associated structural loads of a VLFS, which consists of four modules that are connected to each other by hinged or flexible connectors, were studied by Du and Ertekin (1991). These results showed that the connectors positioned in different locations have different connector loads and thus suggested that one may have to use different connector designs at different locations between modules. Riggs and Ertekin (1993)developed a three-dimensional hydroelastic model of a multi-module floating structure under regular waves in arbitrary angle by using FEM for structures and a strip method for the fluid. The connector is represented by a linearized stiffness matrix with respect to the displacements at the module connection points. Since a refined finite element model for a massive scale of floating structure requires tremendous computing effort, the rigid module flexible connector (RMFC) model was proposed for conceptual and preliminary design. In the RMFC model, the VLFS is represented by rigid modules connected by flexible connectors where the connectors are usually modeled as linear springs with zero-length (Riggs et al., 2000). A floating airport model, consisting of ten identical column-stabilized modules connected by a combination of springs and damping devices, was developed by Paulling and Tyagi (1993). The force of connector device was composed of parts linear proportional to the relative displacement and relative velocity respectively between the modules at the point of connection.

By reviewing the research works above and many others not listed here carefully, we can conclude that almost all of the modeling methods adopt the linearization approach for the classical beam (or plate) models or FEM models for VLFS. When dealing with connector models, it is common to assume the flexible connection as independent linear springs in all degrees of freedom or discretized stiffness matrix using FEM method. In fact, due to the considerable differences in the scale sizes between the floating modules and flexible connectors, small displacements of the floating modules may cause very large displacements at joints of connectors, which give rise to strongly geometrical nonlinearity when establishing the connector model. A compliant connector concept that the braid reinforced elastomeric tubes was used as the compliant element was designed by employing the cable compliant technology (Derstine and Brown, 2000). By using nonlinear finite element method to analyze the stiffness property of the connector, it found that the connector has material and geometric nonlinearity. Fu et al. formulated the motion equations for the flexible connected floating bridge with consideration of the nonlinear properties of connectors and vehicles' inertia effects (Fu et al., 2005). The results showed that nonlinearities and initial gap of the connectors must be taken into account for the nonlinear connected floating bridge since they have an obvious impact on the static deflection, dynamic displacement responses and dynamic connection forces of the bridge. Our recent works about floating airport coupled by rubber-cable connector (Xu et al., 2014b)(Zhang et al., 2015a) and elastic hinge connector(Zhang et al., 2015c) also revealed that the nonlinear stiffness may significantly amplify the module responses and connector loads through jumping phenomena, while the linear methods significantly underestimate the actual module responses and connection loads.

For a floating airport consists of multiple floating modules and these floating modules are elastically coupled by connectors, each module under the excitation of waves can be viewed as an oscillator and the connector can be viewed as coupling. Thus the integrated platform of the connected modules can be regarded as a dynamic network. Based on the nonlinear network theory, our recent research works about the floating airport coupled by rubber-cable connectors (Xu et al., 2014a, 2014b; Zhang et al., 2015a, 2015b) investigated the coupling effect that could significantly influence the dynamics prediction of the floating airport. A verity of complex collective behaviors, such as the transition of module responses and connector loads (Xu et al., 2014a), synchronous phenomena of responses among floating modules and the coupling synergistic effect of network dynamics (Zhang et al., 2015a) were revealed. Among them, a remarkable phenomenon of amplitude death(AD) caught our attention. Amplitude death refers to a special dynamic stability for network system which was first discovered in a chemical reaction (Bar-Eli, 1984). Amplitude death means that all oscillators collectively cease the oscillation in autonomous networks (Saxena et al., 2012) or tend to a suppressed weak oscillatory state in non-autonomous networks (Resmi et al., 2011) due to the interaction among coupled oscillators. More importantly, the amplitude death becomes a new concept for the global dynamic stability of networks. Based on the concept of amplitude death, we can improve the stationary of the floating airport in waves, which means to improve the operating condition of the platform and reduce the connection loads for longer service.

This paper particularly studies the effect of connection configurations based on the amplitude death mechanism. Three new types of connections, including the parallel hinge type, cross hinge type and compound type, are proposed for the investigation. A nonlinear chain-like network model of the floating airport will be developed by integrating the linear wave theory, a dynamic model of single floating module, a mechanics model of the connector and model of a mooring system. The parametric charts of the amplitude death state will be presented for the three types of the connection forms. The comparison and discussion on the dynamic stability of the floating airport will be addressed. The conclusion will be made on the outperformance of the connection form based on the amplitude death mechanism. This work attempts to provide a theoretical guideline for connector design and safety design of the floating airport.

2. Network model of floating airport

Very large floating airport consists of N floating modules coupled by flexible connectors with a chain-type topology, shown in Fig. 1. The global coordinate for the system is defined as x-axis on the undisturbed free-surface plane aligned with the longitudinal direction of the floating airport and the z-axis is upwards. In this paper, the fluid is assumed as ideal liquid and each module is assumed as rigid body and the adjacent modules are coupled by flexible connector, thus the floating airport can be viewed as rigid module flexible connector model, namely RMFC. Only the surge, heave, and pitch motions are considered in this two dimensional model.

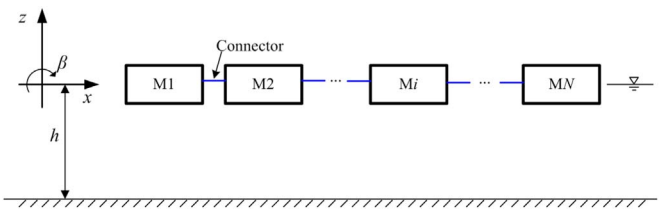

Fig. 1. Sketch of multi-module floating airport.

2.1. Model of single floating body

For a single floating module, by applying the linear wave theory (Stoker, 2011), we can formulate a governing equation of motion for the module, given as

$$(\mathbf{M}_i + \boldsymbol{\mu}_i)\ddot{\mathbf{X}}_i + \boldsymbol{\lambda}_i\dot{\mathbf{X}}_i + \mathbf{S}_i\mathbf{X}_i = \mathbf{F}_i^w + \mathbf{F}_i^c + \mathbf{F}_i^m \tag{1}$$

where $\mathbf{X}_i = (x, z, \beta)^T$ denotes displacement vector of the ith module where x, z, β indicate surge, heave and pitch motions respectively and the superscript T denotes the transpose. The matrices $\mathbf{M}_i$, $\mathbf{S}_i$ denote mass matrix and hydrostatic restoring matrix of the ith module, written as

$$\mathbf{M}_i = \begin{bmatrix} m_i & 0 & m_i(z_{ci} - z_{gi}) \\ 0 & m_i & -m_i(x_{ci} - x_{gi}) \\ m_i(z_{ci} - z_{gi}) & -m_i(x_{ci} - x_{gi}) & I_{xxi}^V + I_{zzi}^V \end{bmatrix} \tag{2}$$

$$\mathbf{S}_i = \begin{bmatrix} 0 & 0 & 0 \\ 0 & \rho g A_i^W & -\rho g I_{xi}^W \\ 0 & -\rho g I_{xi}^W & \rho g(I_{xxi}^W + I_{zzi}^W) - mg(z_{ci} - z_{gi}) \end{bmatrix} \tag{3}$$

where m_i denotes mass of single module. ρ denotes water density and g is the gravitational acceleration. Coordinates (x_{ci}, z_{ci}), (x_{gi}, z_{gi}) indicate the rotational center and gravity center of the ith module respectively. A_i^W indicates the water plane area of the module and satisfied $A_i^W = L_i$ for the two dimensional problem, where L_i denotes the body length of the module. The first and second moment of inertia of water plane area and submerged volume with respect to the rotation center I_{xi}^W, I_{xxi}^W, I_{zzi}^W, I_{xxi}^V, I_{zzi}^V are defined as below (Sannasiraj et al., 2001)

$$I_{xxi}^V = \iint_V (x - x_{ci})^2 dm, \qquad I_{zzi}^V = \iint_V (z - z_{ci})^2 dm$$

$$I_{xxi}^W = \int_{A^W} (x - x_{ci})^2 dA, \qquad I_{zzi}^W = \int_{A^W} (z - z_{ci})^2 dA,$$

$$I_{xi}^W = \int_{A^W} (x - x_{ci}) dA$$

The symbol $\mathbf{F}_i^w$ in the right hand side of Eq. (1) indicates the wave force imposed on the ith module. For a linear head wave of height a, and wave regular frequency $\omega = 2\pi/T$, where T is the wave period, the total wave potential can be separated into incident potential, scattered potential and radiation potential (Stoker, 2011). The matrices $\boldsymbol{\mu}_i$, $\boldsymbol{\lambda}_i$ in Eq. (1) represent the added mass and the added damping matrixes of the ith module respectively as a result of the radiation potential due to the motion of the module, and their elements can be determined by using the eigen-function expansion matching method (Zheng et al., 2004). The wave force $\mathbf{F}^w$ imposed on the floating module can be obtained by integrating the incident potential and scattered potential along its wet surface. The incident and diffraction wave potential mainly contribute to the periodic excitation force, while the effect of scattered wave potential is not considered here for the reason of simplicity and two dimensional problem, as the main attempt in this work is to illustrate the feasibility of the network theory for the dynamic prediction of the floating airport. As for the effect of scattered wave potential, the interested readers can refer a very recent work (Zhang et al., 2015c). Thus the wave force imposed on a single floating module can be written as

$$\mathbf{F}^w = \left[f_{wx}, f_{wz}, f_{w\beta}\right]^T e^{i\omega t} \tag{4}$$

where $i = \sqrt{-1}$ and the amplitudes $f_{wx}, f_{wz}, f_{w\beta}$ of wave force can be obtained by integrating incident wave potential along the wet surface of the module, we obtained,

$$\left.\begin{aligned} f_{wx} &= \rho g a(1 - \cos(kL_i))\frac{\sinh(kh) - \sinh(k(h-d_i))}{k\cosh(kh)} \\ f_{wz} &= \rho g a \sin(kL_i)\frac{\cosh(k(h-d_i))}{k\cosh(kh)} \\ f_{w\alpha} &= \rho g a\left(\frac{\cos(kL_i)}{k^2\cosh(kh)}[kd_i\sinh(k(h-d_i)) + \cosh(k(h-d_i)) - \cosh(kh)]\right. \\ &\left. -\frac{\cosh(k(h-d_i))}{k^2\cosh(kh)}[2\cos\tfrac{kL_i}{2} + 2\cos\tfrac{3kL_i}{2} - kL_i\sin\tfrac{3kL_i}{2}]\right) \end{aligned}\right\} \tag{5}$$

where d_i denotes the sub-depth of the ith module. h indicates water depth, k is a wave number satisfying the dispersion relation $\omega^2 = gk\text{th}kh$.

The last two terms $\mathbf{F}_i^c$, $\mathbf{F}_i^m$ in Eq. (1) indicate the forces imposed on the module due to the flexible connector and the mooring system which will derived latter in details. Since modeling a single floating body is a well-developed method, here we do not intend to involve details of derivation but provide good references for the model terms derived.

2.2. Mechanics model of connectors

Flexible connector is a key element for multi-module floating airport, which significantly influences dynamic characteristics of the floating airport. In this paper, three topological configurations of flexible connectors, including parallel hinge type, cross hinge type and compound type shown in Fig. 2, are proposed for the assessment of dynamic stability of the floating airport.

The three types of connectors are assembled in different configurations by using same linear elastic device show in Fig. 2(a). The elastic device element, like a piston, consists of two linear helical springs, piston rod and sleeve with a rod and the ends of the two rods is spherical hinges, which can connect with the module. For the parallel hinge type connector in Fig. 2(b), the two elastic devices are positioned in parallel with a vertical distance δ_2, for cross hinge type connector in Fig. 2(c), the two elastic devices are positioned in cross and the compound type connector in Fig. 2(d) is the superposition of above two models. For the three types of connectors, the two endpoints of each elastic device are hinged with adjacent modules. The mechanics

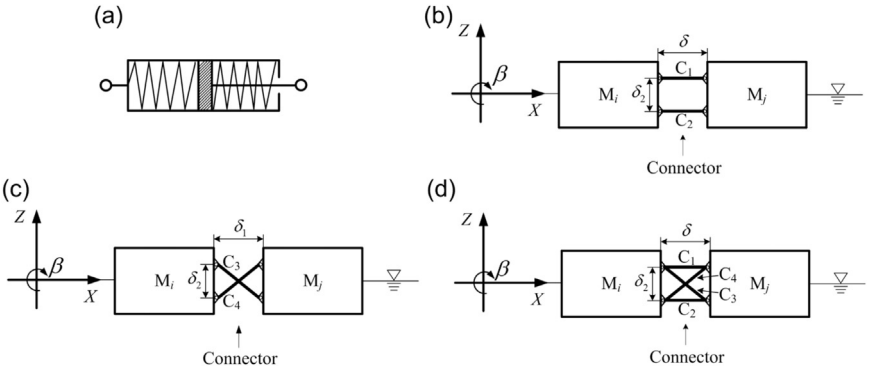

Fig. 2. Sketch for the connectors (a) elastic device element, (b) the parallel hinge connector, (c) the cross hinge connector and (d) the compound connector.

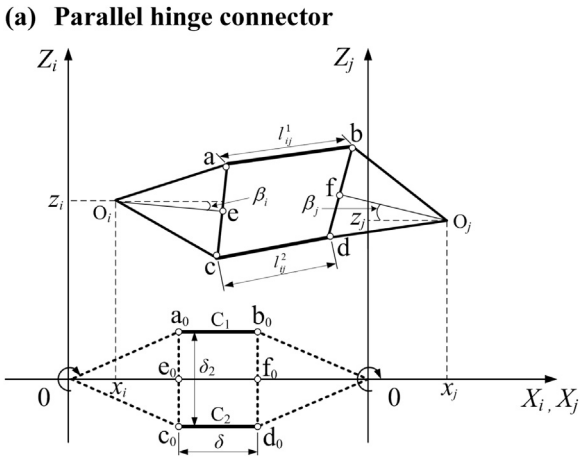

Fig. 3. The position relationship between adjacent modules for parallel hinge connector.

models of the three connectors are formulated below.

Before deriving the mathematical model, we first define a local coordinate (X_i, Z_i) of the ith module below. The rotation center of the resting floating module is defined as the origin of coordinates, X_i axis is parallel to undisturbed free-surface and Z_i axis points upwards. We can simplify the adjacent modules as two triangles. The dashed line triangle denotes the initial position and the solid line one represents the position after the deformation with the displacement (x_i, z_i, β_i) and (x_j, z_j, β_j). The hollow circles denote the hinge joints. The pitch angle β of each module is a small quantity due to the huge scale of the module, so there are

$$\sin\beta \approx \beta, \qquad \cos\beta \approx 1 \tag{6}$$

In what follows, we will formulate the mechanical model of the coupled connectors based on the approximation of Eq. (6).

2.2.1. Parallel hinge connector

For the parallel hinge connector, the sketch of coordinate and the position relationship for adjacent modules is shown in Fig. 3. The two elastic devices denote as C1,C2 and the initial length is δ. Considering the geometric relationship of adjacent modules, the deformation of devices $\Delta l_{ij}^{(k)}$ $(k = 1, 2)$ are formulated as

$$\Delta l_{ij}^{(k)} = l_{ij}^{(k)} - \delta; \quad k = 1, 2 \tag{7}$$

where,

$$l_{ij}^{(1)} = \sqrt{\left[Sgn{\cdot}\delta + \tfrac{\delta_2}{2}(\beta_j - \beta_i) + x_j - x_i\right]^2 + \left[Sgn{\cdot}\tfrac{L}{2}(\beta_j + \beta_i) + z_j - z_i\right]^2}$$

$$l_{ij}^{(2)} = \sqrt{\left[Sgn{\cdot}\delta - \tfrac{\delta_2}{2}(\beta_j - \beta_i) + x_j - x_i\right]^2 + \left[Sgn{\cdot}\tfrac{L}{2}(\beta_j + \beta_i) + z_j - z_i\right]^2}$$

where $Sgn = \mathrm{sgn}(j - i)$ denotes the signum function.

The direction vector for the projection of the elastic devices deformation are formulated as

$$\mathbf{n}_{ij}^{(k)} = \Theta_{ij}^{(k)}\mathbf{i} + \Pi_{ij}^{(k)}\mathbf{k} \tag{8}$$

where $\mathbf{i}$, $\mathbf{k}$ denote the unit vector of x, z axis and $\Theta_{ij}^{(k)}$, $\Pi_{ij}^{(k)}$ denote the deformation coefficients in the surge and heave directions, respectively,

$$\left.\begin{aligned}\Theta_{ij}^{(1)} &= \frac{Sgn\cdot\delta + \frac{\delta_2}{2}(\beta_j - \beta_i) + x_j - x_i}{l_{ij}^{(1)}}, \quad \Pi_{ij}^{(1)} = \frac{Sgn\cdot\frac{L_i}{2}(\beta_j + \beta_i) + z_j - z_i}{l_{ij}^{(1)}}\\ \Theta_{ij}^{(2)} &= \frac{Sgn\cdot\delta - \frac{\delta_2}{2}(\beta_j - \beta_i) + x_j - x_i}{l_{ij}^{(2)}}, \quad \Pi_{ij}^{(2)} = \frac{Sgn\cdot\frac{L_i}{2}(\beta_j + \beta_i) + z_j - z_i}{l_{ij}^{(2)}}\end{aligned}\right\} \tag{9}$$

The vector of force arm imposed on the rotation center of the ith module due to connector forces is formulated as

$$\mathbf{r}_{ij}^{(k)} = r_{ijx}^{(k)}\mathbf{i} + r_{ijz}^{(k)}\mathbf{k} \tag{10}$$

where

$$\left.\begin{aligned}r_{ijx}^{(1)} &= Sgn\cdot\tfrac{L_i}{2} + \tfrac{\delta_2}{2}\beta_i, \quad r_{ijz}^{(1)} = \tfrac{\delta_2}{2} - Sgn\cdot\tfrac{L_i}{2}\beta_i\\ r_{ijx}^{(2)} &= Sgn\cdot\tfrac{L_i}{2} - \tfrac{\delta_2}{2}\beta_i, \quad r_{ijz}^{(2)} = -\tfrac{\delta_2}{2} - Sgn\cdot\tfrac{L_i}{2}\beta_i\end{aligned}\right\} \tag{11}$$

The vector of moment imposed on the rotation center of the ith module due to the connector forces is formulated as

$$\mathbf{m}_{ij}^{(k)} = \mathbf{r}_{ij}^{(k)} \times \mathbf{n}_{ij}^{(k)} = \Upsilon_{ij}^{(k)}\mathbf{j} \tag{12}$$

where $\mathbf{j}$ denotes the unit vector of y axis and $\Upsilon_{ij}^{(k)}$ denotes the deformation coefficients in the pitch direction. Substituting the Eqs. (8) and (10) into Eq. (12), we obtained

$$\Upsilon_{ij}^{(k)} = \Theta_{ij}^{(k)} r_{ijz}^{(k)} - \Pi_{ij}^{(k)} r_{ijx}^{(k)} \tag{13}$$

In this paper, we assume that a single elastic device has a linear stiffness k_c along its longitudinal direction, thus the force of the coupled connectors imposed on the ith module gives,

$$\mathbf{F}_{ij}^{c} = k_c[\Delta u_{ijx} \quad \Delta u_{ijz} \quad \Delta u_{ij\beta}]^T \tag{14}$$

where

$$\Delta u_{ijx} = \Delta l_{ij}^{(1)}\Theta_{ij}^{(1)} + \Delta l_{ij}^{(2)}\Theta_{ij}^{(2)}, \quad \Delta u_{ijz} = \Delta l_{ij}^{(1)}\Pi_{ij}^{(1)} + \Delta l_{ij}^{(2)}\Pi_{ij}^{(2)},$$
$$\Delta u_{ij\beta} = \Delta l_{ij}^{(1)}\Upsilon_{ij}^{(1)} + \Delta l_{ij}^{(2)}\Upsilon_{ij}^{(2)} \tag{15}$$

For this configuration of the connector, it can well resist the relative motion of the surge degree of freedom while it cannot restrict the pitch motion due to a four linkage mechanism.

2.2.2. Cross hinge connector

Similarly, for the cross hinge connector, the sketch of coordinate and the position relationship between adjacent modules is shown in Fig. 4. The two elastic devices denote as C3,C4 and the initial length is $\sqrt{\delta^2 + {\delta_2}^2}$. Considering the geometric relationship of adjacent modules, the deformation of devices $\Delta l_{ij}^{(k)}$ $(k = 3, 4)$ are formulated as

$$\Delta l_{ij}^{(k)} = l_{ij}^{(k)} - \sqrt{\delta^2 + {\delta_2}^2}; \qquad k = 3, 4 \tag{16}$$

where,

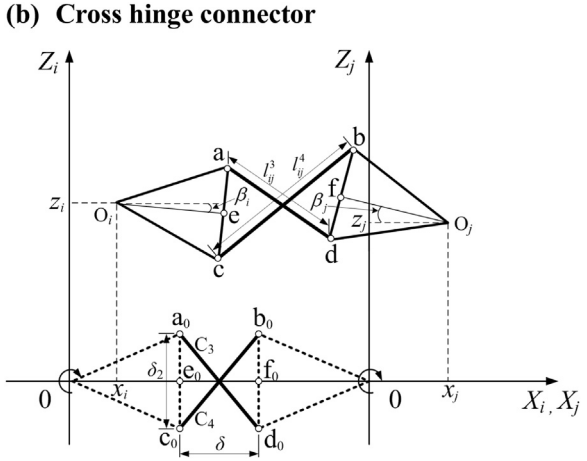

Fig. 4. The position relationship between adjacent modules for cross hinge connector.

$$l_{ij}^{(3)} = \sqrt{\left[Sgn\cdot\delta - Sgn\cdot\frac{\delta_2}{2}(\beta_j+\beta_i) + x_j - x_i\right]^2 + \left[-Sgn\cdot\delta_2 + Sgn\cdot\frac{L}{2}(\beta_j+\beta_i) + z_j - z_i\right]^2}$$

$$l_{ij}^{(4)} = \sqrt{\left[Sgn\cdot\delta + Sgn\cdot\frac{\delta_2}{2}(\beta_j+\beta_i) + x_j - x_i\right]^2 + \left[Sgn\cdot\delta_2 + \mathrm{sgn}(j-i)\frac{L}{2}(\beta_j+\beta_i) + z_j - z_i\right]^2}$$

The direction vector for the projection of the elastic devices deformation are formulated as

$$\mathbf{n}_{ij}^{(k)} = \Theta_{ij}^{(k)}\mathbf{i} + \Pi_{ij}^{(k)}\mathbf{k} \tag{17}$$

where $\Theta_{ij}^{(k)}$, $\Pi_{ij}^{(k)}$ denote the deformation coefficients in the surge and heave directions, respectively,

$$\left.\begin{aligned}\Theta_{ij}^{(3)} &= \frac{Sgn\cdot\delta - Sgn\cdot\frac{\delta_2}{2}(\beta_j+\beta_i) + x_j - x_i}{l_{ij}^3}, \quad \Pi_{ij}^{(3)} = \frac{-Sgn\cdot\delta_2 + Sgn\cdot\frac{L_i}{2}(\beta_j+\beta_i) + z_j - z_i}{l_{ij}^3}\\ \Theta_{ij}^{(4)} &= \frac{Sgn\cdot\delta + Sgn\cdot\frac{\delta_2}{2}(\beta_j+\beta_i) + x_j - x_i}{l_{ij}^4}, \quad \Pi_{ij}^{(4)} = \frac{Sgn\cdot\delta_2 + Sgn\cdot\frac{L_i}{2}(\beta_j+\beta_i) + z_j - z_i}{l_{ij}^4}\end{aligned}\right\} \tag{18}$$

The vector of force arm imposed on the rotation center of the ith module due to connector forces is formulated as

$$\mathbf{r}_{ij}^{(k)} = r_{ijx}^{(k)}\mathbf{i} + r_{ijz}^{(k)}\mathbf{k} \tag{19}$$

where

$$\left.\begin{aligned}r_{ijx}^{(3)} &= Sgn\cdot[\tfrac{L}{2} + \tfrac{\delta_2}{2}\beta_i], \quad r_{ijz}^{(3)} = Sgn\cdot[\tfrac{\delta_2}{2} - \tfrac{L}{2}\beta_i]\\ r_{ijx}^{(4)} &= Sgn\cdot[\tfrac{L}{2} - \tfrac{\delta_2}{2}\beta_i], \quad r_{ijz}^{(4)} = Sgn\cdot[-\tfrac{\delta_2}{2} - \tfrac{L}{2}\beta_i]\end{aligned}\right\} \tag{20}$$

The vector of moment imposed on the rotation center of the ith module due to the connector forces is formulated as

$$\mathbf{m}_{ij}^{(k)} = \mathbf{r}_{ij}^{(k)} \times \mathbf{n}_{ij}^{(k)} = \Upsilon_{ij}^{(k)}\mathbf{j} \tag{21}$$

where $\Upsilon_{ij}^{(k)}$ denotes the deformation coefficients in the pitch direction. Substituting the Eqs. (8) and (10) into Eq. (12), we obtained

$$\Upsilon_{ij}^{(k)} = \Theta_{ij}^{(k)} r_{ijz}^{(k)} - \Pi_{ij}^{(k)} r_{ijx}^{(k)} \tag{22}$$

In this paper, we assume that a single connector has a linear stiffness k_c along its longitudinal direction, thus the force of the coupled connectors imposed on the ith module gives,

$$\mathbf{F}_{ij}^{c} = k_c[\Delta v_{ijx} \quad \Delta v_{ijz} \quad \Delta v_{ij\beta}]^T \tag{23}$$

where

$$\Delta v_{ijx} = \Delta l_{ij}^{(3)}\Theta_{ij}^{(3)} + \Delta l_{ij}^{(4)}\Theta_{ij}^{(4)}, \quad \Delta v_{ijz} = \Delta l_{ij}^{(3)}\Pi_{ij}^{(3)} + \Delta l_{ij}^{(4)}\Pi_{ij}^{(4)},$$
$$\Delta v_{ij\beta} = \Delta l_{ij}^{(3)}\Upsilon_{ij}^{(3)} + \Delta l_{ij}^{(4)}\Upsilon_{ij}^{(4)} \tag{24}$$

For this configuration of the connector, the constraint for heave motion is enhanced due to the inclined device in comparison with parallel hinge connector.

2.2.3. Compound connector

For the compound connector, it is the superposition of the parallel and cross hinge connectors, thus the mechanics model can be derived by using superposition theory and it can performance the compound characteristics of the above two connection types (Fig. 5).

Similarly, we assume that a single elastic device has a linear stiffness k_c along its longitudinal direction, thus the force of the coupled connectors imposed on the ith module gives,

$$\mathbf{F}_{ij}^{c} = k_c[\Delta u_{ijx} + \Delta v_{ijx} \quad \Delta u_{ijz} + \Delta v_{ijz} \quad \Delta u_{ij\beta} + \Delta v_{ij\beta}] \tag{25}$$

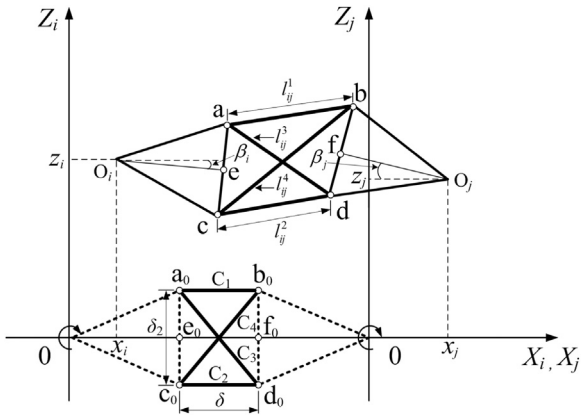

Fig. 5. The position relationship between adjacent modules for compound connector.

By now, we have derived the mechanical models for three types of flexible connectors in Eqs. (14), (23) and (25). Note that the models of the connectors all contain nonlinear geometric characteristic. Also note that the displacements at the hinge joints are usually large even if the pitch angles of the modules are small due to the huge scale of the module. Thus the models of the connectors present strong nonlinearity. On the other hand, the stiffness of the connection between adjacent modules in a specified degree of freedom depends on the motions in other degrees of freedom even if the stiffness of the elastic device possesses a linear property.

2.3. Constraint model of mooring system

To prevent drifting, the floating structure is practically constrained by a mooring system. Various types of mooring systems are proposed by scholars over the past few decades. In this paper, we choose a slack catenary line of simple mooring system in this paper, shown in Fig. 6. It assumed that the mooring line is perfectly flexible, inextensible and heave. Thus, the linearized stiffness coefficients can be formulated as (Sannasiraj et al., 1998)

$$\left.\begin{aligned}k_{xx} &= \frac{w\sinh\eta}{\eta\sinh\eta - 2(\cosh\eta - 1)}\\ k_{zz} &= w\eta\\ k_{\alpha\alpha} &= (\tfrac{L}{2})^2 w\eta\\ k_{xz} &= \frac{w(1-\cosh\eta)}{\eta\sinh\eta - 2(\cosh\eta - 1)}\\ k_{zx} &= \frac{w\cosh\eta(\cosh\eta - 1)}{\eta\sinh\eta - 2(\cosh\eta - 1)}\\ k_{x\alpha} &= k_{\alpha x} = 0\\ k_{z\alpha} &= k_{\alpha z} = \frac{L}{2}w\eta\end{aligned}\right\} \tag{26}$$

where $\eta = s/c$, $c = Q/w$. w denotes unit weight of catenary line. Generally, the length H_0 of mooring line, anchoring distance s_0 and water depth h are known. The length of suspending segment of catenary line H and corresponding projective length to the seabed s

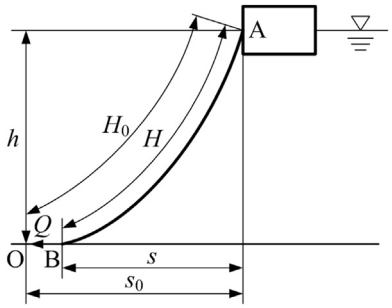

Fig. 6. Sketch of mooring line constraint.

are unknown which can be calculated from equation of static equilibrium (Ogawa, 1984). Thus, the mooring stiffness matrix can be calculated using Eq. (26). The force of mooring lines imposed on floating modules can be defined as

$$\mathbf{F}^m = -\mathbf{KX} \tag{27}$$

2.4. Network model of multi-module floating airport

In above sections, we have formulated the individual models of the key parts of the floating airport. We now can integrate the sub-models to form a network model of multi-module floating airport step by step.

Considering a head wave propagates along the huge size of the floating airport, the wave forces imposed on the adjacent modules should have a phase difference, so that combined with wave force in Eq. (4), the wave forces imposed on the i-th module can be formulated as

$$\mathbf{F}_i^w = \mathbf{F}^w e^{i\varphi_i} \tag{28}$$

where φ_i is initial phase angle of the ith module which satisfies $\Delta\varphi_{i(i+1)} = \varphi_{i+1} - \varphi_i = \frac{k}{2}(L_i + L_{i+1})$ comparing the length of the wave and the module.

Due to the multi-functional specialty, very large floating structure can be integrated via different topology shapes, such as chain-type for a floating runway (June Bai et al., 2001), rectangular-type for entertainment facilities (Koh and Lim, 2009), circular-type for a artificial islands (Andrianov and Hermans, 2005). In order to deal with various topology structures for VLFS, we introduce a topology matrix $\Phi \in R^{N\times N}$ where its element Φ_{ij} is set to 1 when the ith module connects with the jth module, otherwise Φ_{ij} is set to zero. The diagnose element Φ_{ii} is also set to zero which means that a module cannot connect with itself. Because of multiple modules connected together and considering the mechanical model Eqs. (14),(23) and (25) of three connector types, the total connector force imposed on the ith module can be formulated as

$$\mathbf{F}_i^c = \sum_{j=1}^{N} \Phi_{ij}\mathbf{F}_{ij}^c \tag{29}$$

Introducing the topology matrix into the dynamics model is one of the advantages of network theory which can deal with the connection of arbitrary topology of network structures by only changing the element assignment. It is worth noting that for the different types of topology network, such as a ring form or a rectangular form, we can formulate the models only by assigning the elements value of the topology matrix accordingly.

Considering the effect of mooring system, and in order to deal with flexibility of mooring position, the mooring force imposed on the ith module can be formulated as

$$\mathbf{F}_i^m = \delta(i, i_0)\mathbf{F}^m \tag{30}$$

where $\delta(i, i_0)$ is the Delta function and i_0 denotes the number of module on which the mooring system acts.

For a multi-module floating airport with N modules, the generalized network dynamic model can be derived by integrating the model of single floating body in Eq. (1), wave force model in Eq. (28), mechanics model of connector (29) and the model of mooring system in Eq. (30), written as,

$$(\mathbf{M}_i + \boldsymbol{\lambda}_i)\ddot{\mathbf{X}}_i + \boldsymbol{\mu}_i\dot{\mathbf{X}}_i + (\mathbf{S}_i + \delta(i, i_0)\mathbf{K}_i)\mathbf{X}_i = \mathbf{F}^w e^{i\varphi_i} + \varepsilon \sum_{j=1}^{N} \Phi_{ij}G(\mathbf{X}_i, \mathbf{X}_j),$$
$$i = 1, \ldots, N \tag{31}$$

where the terms in left hand of Eq. (31) are explicit, the last term $\varepsilon \sum_{j=1}^{N} \Phi_{ij}G(\mathbf{X}_i, \mathbf{X}_j)$ denotes the coupling term which represents the mechanical features of the connection between the modules. The parameter ε indicate coupling strength corresponding to the stiffness of connector, $G(\mathbf{X}_i, \mathbf{X}_j)$ is referred as the coupling function in network theory which defines the specific interaction form and material property of the connector in all degrees of freedom. In this paper, the coupling function $G(\mathbf{X}_i, \mathbf{X}_j)$ corresponding to the three types of connectors can be expressed respectively, for the parallel hinge connector is

$$G(\mathbf{X}_i, \mathbf{X}_j) = [\Delta u_{ijx} \quad \Delta u_{ijz} \quad \Delta u_{ij\beta}]^T \tag{32}$$

for the cross hinge connector, there have

$$G(\mathbf{X}_i, \mathbf{X}_j) = [\Delta v_{ijx} \quad \Delta v_{ijz} \quad \Delta v_{ij\beta}]^T \tag{33}$$

and for the compound connector, written as

$$G(\mathbf{X}_i, \mathbf{X}_j) = [\Delta u_{ijx} + \Delta v_{ijx} \quad \Delta u_{ijz} + \Delta v_{ijz} \quad \Delta u_{ij\beta} + \Delta v_{ij\beta}]^T \tag{34}$$

The coupling function here basically describes the nonlinear geometric relationship for the connectors.

By now, a standard procedure for establishing the network model of a floating airport is demonstrated. It's worthy to notice that the modeling method is not only suitable for the floating airport but also available to other engineering problems with network structure alike.

3. Amplitude death stability of floating airport

Safety of floating airport is an important aspect in engineering design, where the system stability is greatly concerned. In this paper, different from traditional methods, we assess the stability of the floating airport based on the new concept of amplitude death that refers to as a suppressed weak oscillatory state in network theory. Amplitude death corresponds to a stationary state of the floating airport, and is a crucial index to assess the stability performance of the floating system in waves. Firstly, the phenomena of amplitude death for the three types of connectors are illustrated by numerical simulations using Runge-Kutta method (ode45 in Matlab) to guarantee the numerical stability. Then, the parametric domains for the onset of amplitude death are presented in conjunction with the three different types of connectors, from which we can evaluate the effect of the connector designs in terms of the AD stability.

3.1. Simulation parameters

In this paper, a chain-type floating airport that consists of five equal-sized modules coupled by flexible connector is chosen for the simulation model. Rigid mat-type module is considered and its properties are listed in Table 1. The parameters for the wave are of wave height $a = 3$m, namely 5 sea state, and wave period $8 - 20$s, which can cover the wave spectrum range of general sea state. Water depth is $h = 50$m.

According to the proposed three types of connectors, three simulation models of the floating airport are shown in Fig. 7. For the chain-type network model of the floating airport, the topology matrix Φ_{ij} is symmetric, given by,

$$\Phi_{ij} = \begin{cases} 1 & j = i+1 \\ 0 & others \end{cases} \qquad i = 1, 2, \ldots, N; \quad j = i, i+1, \ldots, N \tag{35}$$

The initial gap between adjacent modules is set at $\delta = 5$m for the three models, and the vertical distance between hinge points is of

Table 1
Particulars of single floating body.

Length L (m)	Height D (m)	Sub-depth d (m)	Mass of unit length m_0 (kg/m)
200	8	5	5125

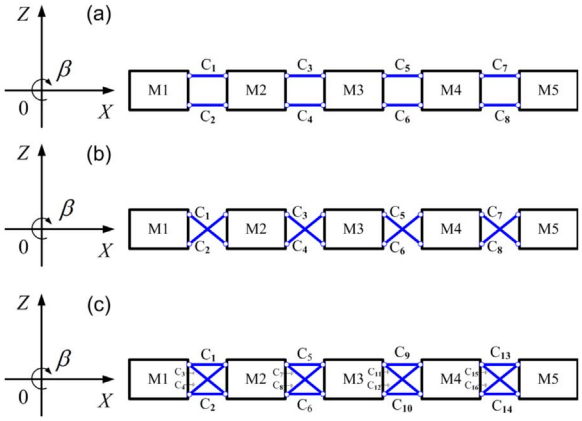

Fig. 7. Configuration sketch of 5-module floating airport (a) for the parallel hinge connector, (b) the cross hinge connector and (c) the compound connector.

$\delta_2 = 5$m. Since all elastic devices of connectors have no pre-tensioning force, so the initial length of the elastic device of connectors can be obtained through the geometrical relationship.

We consider the mooring condition that catenary mooring lines are symmetrically attached to the head and the tail of the chain-topology floating structure. The parameters for the mooring system are set at the unit weight of catenary line $w = 332$kgf, length $H = 135$m, projective length $s_0 = 95$m (Winkler et al., 1990).

3.2. Phenomenon of amplitude death

Fig. 8 illustrates the responses of surge, heave and pitch motion versus connector stiffness for the parallel hinge connector model with a fixed wave period $T = 10$s. From Fig. 8(a)-(c), we can see that the amplitude responses in all degrees of freedom for all modules stays at relatively weak oscillation state when the connection stiffness $k_c < 0.515 \times 10^5$N/m and the amplitudes are simultaneously amplified at a critical value of the coupling strength $k_c = 0.515 \times 10^5$N/m. With the increase of connector stiffness, the responses for all modules tend to significantly large, illustrated by messy dashed lines, which means that the system evolves into chaotic motions or high order harmonic motions. The responses suddenly jump down after the second critical stiffness value of $k_c = 1.42 \times 10^5$N/m, trapped into a relatively weak oscillation. According to the definition of amplitude death for non-autonomous systems (Resmi et al., 2011), the weak oscillation in the intervals of $k_c < 0.515 \times 10^5$N/m and $k_c > 1.42 \times 10^5$N/m are regarded as amplitude death which corresponds to a stationary state of the floating airport. Compared with low and high level oscillation states, the amplitude is enlarged more than 10 times for surge motion, 6 times for heave motion and 8 times for pitch motion, which extremely threatens the safety of the floating airport. The mechanism of amplitude death for non-autonomous system was studied in our recent work (Xu et al., 2014b). Since the system response possesses multiple stabilities, the occurrence of amplitude death is because the system state resides onto a low-level oscillatory solution branch. Due to the synergetic effect for the network system, the critical jump points are identical in all degrees of freedom for all modules, and the motion patterns of all modules are the same at the same parameter settings.

Fig. 9 gives the responses versus connector stiffness for the models of the cross hinge connector and the compound connector. Due to the synergetic effect, only surge motion is shown here. The parameter regions of large oscillation state are $0.89 \times 10^5 < k_c < 2.78 \times 10^5$N/m for the cross hinge connector in Fig. 9(a) and

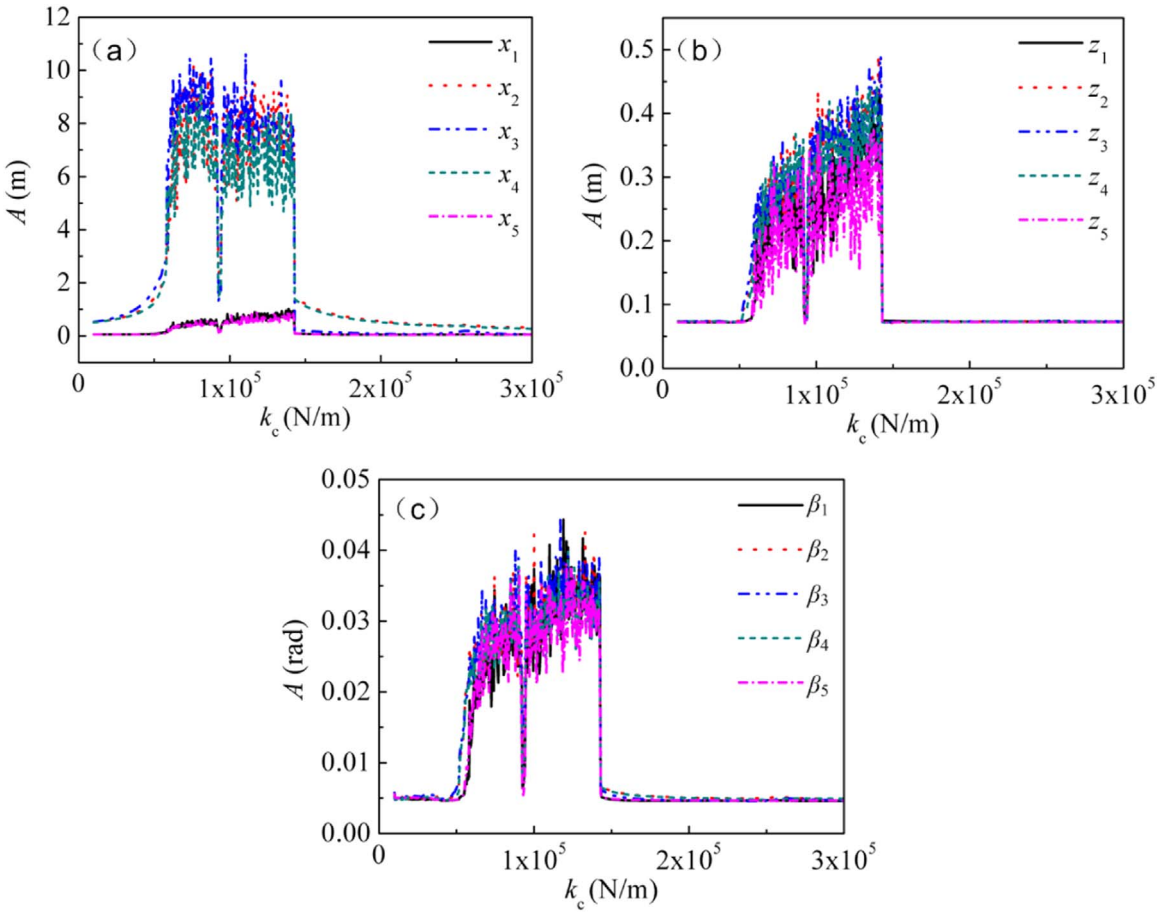

Fig. 8. The response amplitude versus connector stiffness for parallel hinge connector for (a) surge motion, (b) heave motion and (c) pitch motion ($T = 10$s).

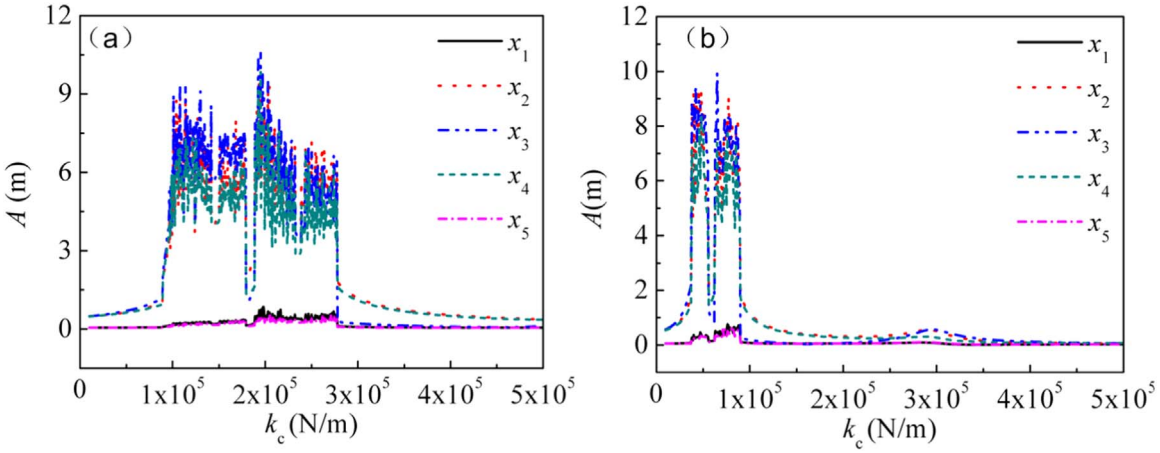

Fig. 9. The response amplitude versus connector stiffness for surge motion (a) with cross hinge connector and (b) with compound connector (T = 10s).

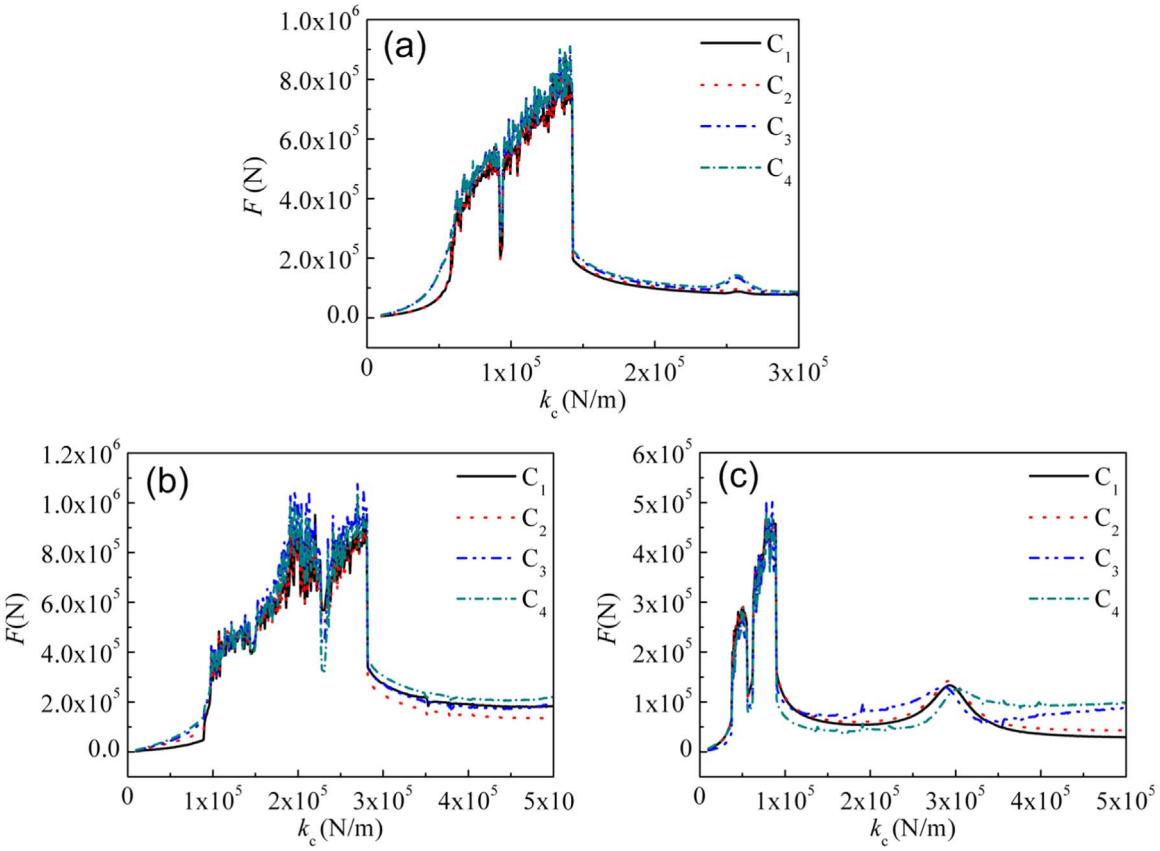

Fig. 10. Connector loads under the change of connector stiffness for (a) parallel hinge connector, (b) cross hinge connector and (c) compound connector (T = 10s).

$0.37 \times 10^5 < k_c < 0.9 \times 10^5$N/m for the compound connector in Fig. 9(b). There exists a weak resonance peak in the vicinity of connector stiffness $k_c = 3 \times 10^5$N/m for the compound connector in Fig. 9(b) but its amplitude still remains small comparing to the high-rise motions after the jump up. In comparison with the surge motion among the three types of connectors, we can find that the connection design has a significant effect on dynamic response. By inspecting Fig. 8(a), Fig. 9(a) and Fig. 9(b), the model of the compound connector occupies the most wider region of stationary state, and followed is the parallel hinge connector, while the cross hinge connector covers the least parametric region for the stationary state. From the geometric layout, we know that the parallel elastic devices mainly provide force in surge direction while the devices installed with the cross layout provide restoring moment for pitch motion principally and can improve the constraint for the heave motion. Thus, the compound connector can provide constraint forces in all three degrees of freedom and delivers superior performance for dynamic response of the floating airport.

Except dynamic responses, connector loads are also concerned for the safety design of the floating airport. Fig. 10 illustrates the connector loads evolution under the change of connector stiffness with a fixed wave period T = 10s.

From Fig. 10, we can see that the evolution of connector loads is similar with motion pattern for responses. The connector loads tend to relative small in the amplitude death region for the three connector forms. In terms of the peak load, the parallel hinge connector and the cross hinge connector are about at the same level, while the compound connector is only half of them.

According to above analysis we can remark that the state of

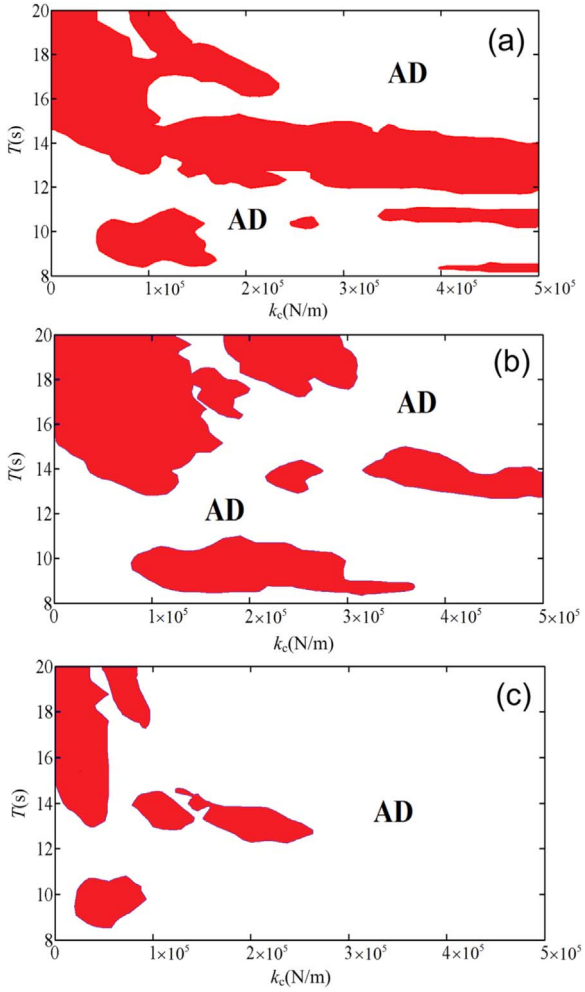

Fig. 11. Parameter domain (k_c, T) for the onset of amplitude death where the white regions labeled as AD that corresponds to weak oscillatory states with wave height $a = 3$m for (a) the parallel hinge connector, (b) cross hinge connector and (c) compound connector.

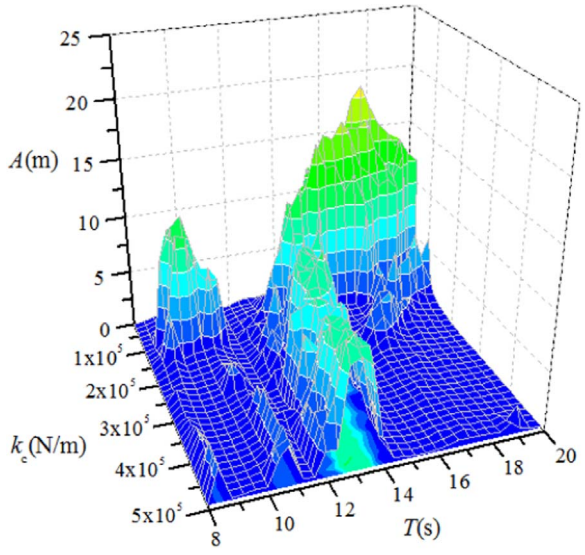

Fig. 12. Amplitude response of surge motion for second module of in parameter space (k_c, T).

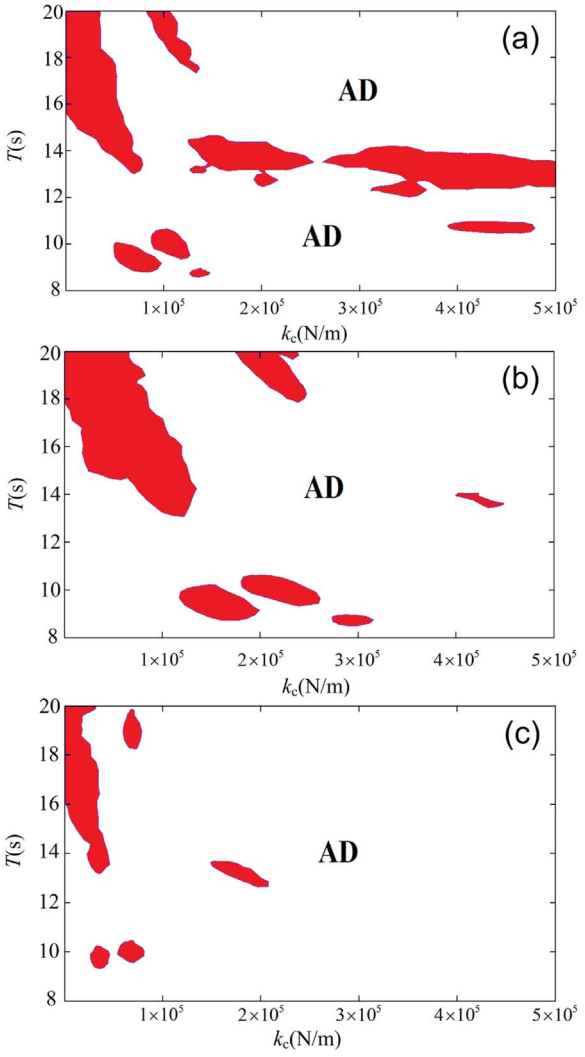

Fig. 13. Parameter domains (k_c, T) of amplitude death for wave height $a = 1$m where the regions labeled as AD correspond to weak oscillatory states for (a) the parallel hinge connector, (b) cross hinge connector and (c) compound connector.

amplitude death is significant for the stability of the floating airport because it enables the system reside in a calm state meanwhile remains the connector load at low level. In addition, the connection configuration has a great effect on the dynamic responses especially for the region of amplitude death.

3.3. Parameter domain of amplitude death stability

Since amplitude death represents the network stability, we are very interested in the distribution of the amplitude death state in a parameter domain because it may provide a valuable guidance for the design of the system stability and safety. The parametric domain is spanned by the connector stiffness and the wave period, where the former takes into the effect of the design of the connectors, and the later reflects the effect of the environmental condition. Because of the network synergistic effect that the responses of all modules in all degrees of freedom have the same oscillation patterns, the AD behavior of the surge motion of the first module can represent the AD behaviors of others. Thus, amplitude death in the following figures is obtained via the motion of surge.

Fig. 11 illustrates the amplitude death regions in the parameter plane (k_c, T). The white region labeled with 'AD' denotes amplitude death state and the red region refers to large oscillation state. Fig. 11(a)

shows the distribution of the amplitude death state for the parallel hinge connector, where a large red band is continuously across over the whole parametric domain of the stiffness. There are some small islands and strips allocated below the red band. The red band mainly appears in the wave period about $12 \leq T \leq 15$s, which means no matter what connector stiffness is set, the AD state cannot be expected in this wave condition. When further examining the configuration of the parallel hinge connector between the adjacent modules, we find that the connection forms a four linkage mechanism that cannot restrict the pitch motion well. Thus we believe that the four linkage connection mechanism may give rise to the large oscillation responses in the red parametric domain. Viewing the diagram of AD domain for the cross hinge connector shown in Fig. 11(b), the large red islands mainly locate at left-top corner and bottom, meaning that large oscillatory state may easily turn up in low and high wave periods. Another feature is that the red region is disconnected in comparison with the results in Fig. 11(a), which conveys a meaningful clue that whatever the wave condition is, we can always find a suitable stiffness to set the floating structure in an AD state. From Fig. 11(c), we can find that the AD region expands greatly and the red islands shrink. Red regions mainly locate on the right-hand side and are not connected. In comparison with the results of the three types of connectors, we can remark that the compound connector outperforms in the amplitude death stability of the floating airport. It implies that the constraint moment for the pitch motion is a key factor for the connector to achieve the better AD stability.

In order to understand the meanings of AD region more, we plot a 3D diagram for the amplitude response of the surge motion of the second module for the floating airport coupled with the parallel hinge connector, shown in Fig. 12. It provides a "geographic" map to view the distribution of amplitude response. In comparison with the corresponding parametric domain of AD shown in Fig. 11(a), we can see that the AD region corresponds to the weak oscillation state colored in blue (like a deep blue sea), and the red region corresponds to the large oscillation state (like sharply right-up cliffs and mountains). Due to the synergetic effect for the network system, other degrees of freedom for different modules all have the similar corresponding relationship. It clearly illustrates that the transition of dynamics from the weak oscillation state to the strong oscillation state is sudden and sharp.

In realistic ocean environment, the wave condition changes frequently. We are also interested in the effect of wave height on the AD state. Fig. 13 illustrates the AD region for wave height $a = 1$m where the white region is marked with 'AD' and the red region stands for high-rise motion state similarly. Compared with the results for wave height $a = 3$m shown in Fig. 11, the skeleton pattern of AD regions are similar but red spots are greatly reduced. As the wave height decreases, the AD region obviously expands over the whole parameter domain.

4. Conclusions

In the present paper, a generalized chain-like nonlinear network model for a floating airport is developed based on the linear wave theory which can deal with arbitrary connector forms. Three novel types of connectors, parallel hinge connector, cross hinge connector and compound connector, are proposed together with the mechanics constitutive models derived. By means of numerical simulations, we study the amplitude death phenomenon of the floating airport in conjunction with the three different connectors. The parametric domain for the amplitude death state is numerically studied in a span of connector stiffness and the wave period. The effect of connector forms on the distribution of the amplitude death state is also discussed. Further, the effect of wave height on the parameters domain of amplitude death of the floating airport is analyzed. Numerical results show that the connector configurations play significant role on the dynamic stability of the floating airport. The inclined elastic elements in the compound connector provide a constraint in the rotational degree of freedom, which greatly reduces the oscillation of the floating airport. This work presents an application example to improve the connector design of the floating airport in terms of amplitude death stability. Nevertheless, we have to note that the results ignoring scattered wave are conservative and only the numerical simulation still cannot draw a convinced conclusion which needs to be experimentally verified in our future work.

Acknowledgments

This research work was supported by the 973 research grant (2013CB036104) and the National Natural Science Foundation of China (11472100).

References

Andrianov, A.I., Hermans, A.J., 2005. Hydroelasticity of a circular plate on water of finite or infinite depth. J. Fluids Struct. 20, 719–733. http://dx.doi.org/10.1016/j.jfluidstructs.2005.03.002.

Armstrong, E.R., 1924. Sea station. 1511153.

Armstrong, E.R., 1943. The seadrome project for transatlantic airways. Seadrome Patents Co, Wilmington.

Bar-Eli, K., 1984. Coupling of chemical oscillators. J. Phys. Chem. 88, 3616–3622. http://dx.doi.org/10.1021/j150660a048.

Derstine, M.S., Brown, R.T., 2000. A compliant connector concept for the mobile offshore base. Mar. Struct. 13, 399–419. http://dx.doi.org/10.1016/S0951-8339(00)00017-4.

Du, S.X., Ertekin, C.R., 1991. Dynamic Response Analysis of A Flexibly Joined, Multi-module Very Large Floating Structure, In: OCEANS 91 Proceedings. IEEE, pp. 1286–1293. doi:http://dx.doi.org/10.1109/OCEANS.1991.606474

Ertekin, R.C., Riggs, H.R., 1991. (Eds.). In: Proceedings of the First International Workshop on Very Large Floating Structures, VLFS'91. Honolulu, HI.

Ertekin, R.C., Kim, J.W., 1999.In: Proceedings of the Third International Workshop on Very Large Floating Structures (VLFS'99): September 22-24, 1999, Honolulu, Hawaii, USA. SOEST, University of Hawaii at Manoa.

Fu, S., Cui, W., Chen, X., Wang, C., 2005. Hydroelastic analysis of a nonlinearly connected floating bridge subjected to moving loads. Mar. Struct. 18, 85–107. http://dx.doi.org/10.1016/j.marstruc.2005.05.001.

Fujikubo, M., Suzuki, H., 2015. Mega-Float. In: Wang, C.M., Wang, B.T. (Eds.), Large Floating Structures. Springer-Verlag, Singapur, 197–219. http://dx.doi.org/10.1007/978-981-287-137-4.

Gao, R.P., Tay, Z.Y., Wang, C.M., Koh, C.G., 2011. Hydroelastic response of very large floating structure with a flexible line connection. Ocean Eng. 38, 1957–1966. http://dx.doi.org/10.1016/j.oceaneng.2011.09.021.

Haeda, H., Miyajima, S., Masuda, K., Ikoma, T., 1996. Hydroelastic responses of pontoon type very large floating offshore structure. American Society of Mechanical Engineers, New York, NY (United States).

Isobe, E., 1999.Research and development of Mega-Float, In: Proceedings of the 3rd International Workshop on Very Large Floating Structures, Honolulu, Hawaii, USA. pp. 7–13.

June Bai, K.,, Suk Yoo, B., Whan Kim, J., 2001. A localized finite-element analysis of a floating runway in a harbor. Mar. Struct. 14, 89–102. http://dx.doi.org/10.1016/S0951-8339(00)00030-7.

Koh, H.S., Lim, Y.B., 2009. The floating platform at the marina Bay, Singapore. Struct. Eng. Int 19, 33–37. http://dx.doi.org/10.2749/101686609787398263.

Maeda, H., Maruyama, S., Inoue, R., Watanabe, K., Togawa, S., Suzuki, F., 1979. On the motions of a floating structure which consists of two or three blocks with rigid or pin joints. J. Soc. Nav. Archit. Jpn. 1979, 71–78. http://dx.doi.org/10.2534/jjasnaoe1968.1979.71.

McAllister, K.R., 1997. Mobile offshore bases—an overview of recent research. J. Mar. Sci. Technol. 2, 173–181. http://dx.doi.org/10.1007/BF02489808.

Michailides, C., Loukogeorgaki, E., Angelides, D.C., 2013. Response analysis and optimum configuration of a modular floating structure with flexible connectors. Appl. Ocean Res. 43, 112–130. http://dx.doi.org/10.1016/j.apor.2013.07.007.

Ogawa, Y., 1984. Fundamental analysis of deep sea mooring line in static equilibrium. Appl. Ocean Res. 6, 140–147. http://dx.doi.org/10.1016/0141-1187(84)90003-8.

Paulling, J.R., Tyagi, S., 1993. Multi-module floating ocean structures. Mar. Struct. 6, 187–205. http://dx.doi.org/10.1016/0951-8339(93)90019-Y.

Resmi, V., Ambika, G., Amritkar, R.E., 2011. General mechanism for amplitude death in coupled systems. Phys. Rev. E 84, 46212. http://dx.doi.org/10.1103/PhysRevE.84.046212.

Riggs, H.R., Ertekin, R.C., 1993. Approximate methods for dynamic response of multi-module floating structures. Mar. Struct. 6, 117–141. http://dx.doi.org/10.1016/0951-8339(93)90016-V.

Riggs, H.R., Ertekin, R.C., Mills, T.R.J., 2000. A comparative study of RMFC and FEA models for the wave-induced response of a MOB. Mar. Struct. 13, 217–232. http://dx.doi.org/10.1016/S0951-8339(00)00029-0.

Sannasiraj, S.A., Sundar, V., Sundaravadivelu, R., 1998. Mooring forces and motion responses of pontoon-type floating breakwaters. Ocean Eng. 25, 27–48. http://dx.doi.org/10.1016/S0029-8018(96)00044-3.

Sannasiraj, S.A., Sundaravadivelu, R., Sundar, V., 2001. Diffraction–radiation of multiple floating structures in directional waves. Ocean Eng. 28, 201–234. http://dx.doi.org/

10.1016/S0029-8018(99)00066-9.
Saxena, G., Prasad, A., Ramaswamy, R., 2012. Amplitude death: the emergence of stationarity in coupled nonlinear systems. Phys. Rep. 521, 205–228. http://dx.doi.org/10.1016/j.physrep.2012.09.003.
Stoker, J.J., 2011. Water waves: the mathematical theory with applications. Wiley-Interscience.
Suzuki, H., 2001. Safety target of very large floating structure used as a floating airport. Mar. Struct. 14, 103–113. http://dx.doi.org/10.1016/S0951-8339(00)00025-3.
Suzuki, H., Riggs, H.R., Fujikubo, M., Shugar, T.A., Seto, H., Yasuzawa, Y., Bhattacharya, B., Hudson, D.A., Shin, H., 2007.Very large floating structures, In: ASME 2007 Proceedings of the 26th International Conference on Offshore Mechanics and Arctic Engineering. American Society of Mechanical Engineers, pp. 597–608.
Watanabe, E., Utsunomiya, T., Wang, C.M., 2004. Hydroelastic analysis of pontoon-type VLFS: a literature survey. Eng. Struct. 26, 245–256. http://dx.doi.org/10.1016/j.engstruct.2003.10.001.
Winkler, R.S., Seidl, L.H., Riggs, H.R., 1990. The design and analysis of very large floating structures. Department of Ocean Engineering, University of Hawaii, Hawaii.
Xia, D., Kim, J.W., Ertekin, R.C., 2000. On the hydroelastic behavior of two-dimensional articulated plates. Mar. Struct. 13, 261–278. http://dx.doi.org/10.1016/S0951-8339(00)00028-9.
Xu, D.L., Zhang, H.C., Lu, C., Qi, E.R., Hu, J.J., Wu, Y.S., 2014a. On Study of Nonlinear Network Dynamics of Flexibly Connected Multi-Module Very Large Floating Structures. (Vulnerability, Uncertainty, and Risk)In: . American Society of Civil Engineers, Reston, VA, 1805–1814. http://dx.doi.org/10.1061/9780784413609.181.
Xu, D.L., Zhang, H.C., Lu, C., Qi, E.R., Tian, C., Wu, Y.S., 2014b. Analytical criterion for amplitude death in nonautonomous systems with piecewise nonlinear coupling. Phys. Rev. E 89, 42906. http://dx.doi.org/10.1103/PhysRevE.89.042906.
Zhang, H.C., Xu, D.L., Xia, S.Y., Lu, C., Qi, E.R., Tian, C., Wu, Y.S., 2015c. Nonlinear network modeling of multi-module floating structures with arbitrary flexible connections. J. Fluids Struct. 59, 270–284. http://dx.doi.org/10.1016/j.jfluidstructs.2015.09.012.
Zhang, H.C., Xu, D.L., Lu, C., Qi, E.R., Hu, J.J., Wu, Y.S., 2015a. Amplitude death of a multi-module floating airport. Nonlinear Dyn. 79, 2385–2394. http://dx.doi.org/10.1007/s11071-014-1819-x.
Zhang, H.C., Xu, D.L., Lu, C., Xia, S.Y., Qi, E.R., Hu, J.J., Wu, Y.S., 2015b. Network dynamic stability of floating airport based on amplitude death. Ocean Eng. 104, 129–139. http://dx.doi.org/10.1016/j.oceaneng.2015.05.008.
Zhang, H.C., Xu, D.L., Xia, S.Y., Qi, E.R., Tian, C., Wu, Y.S., 2015c.Nonlinear Network dynamic characteristics of multi-module floating airport with flexible connectors, In: Proceedings of the Twenty-Fifth (2015) International Ocean and Polar Engineering Conference. Kona, Big Island, Hawaii, USA, pp. 1583–1590.
Zheng, Y.H., You, Y.G., Shen, Y.M., 2004. On the radiation and diffraction of water waves by a rectangular buoy. Ocean Eng. 31, 1063–1082. http://dx.doi.org/10.1016/j.oceaneng.2003.10.012.